

RENORMALIZATION GROUP FLOWS IN SIGMA-MODELS  
COUPLED  
TO TWO-DIMENSIONAL DYNAMICAL GRAVITY

S. Penati <sup>\*</sup>, A. Santambrogio <sup>†</sup> and D. Zanon <sup>‡</sup>

*Dipartimento di Fisica dell' Università di Milano and  
INFN, Sezione di Milano, Via Celoria 16, I-20133 Milano, Italy*

**Abstract**

We consider a bosonic  $\sigma$ -model coupled to two-dimensional gravity. In the semiclassical limit,  $c \rightarrow -\infty$ , we compute the gravity dressing of the  $\beta$ -functions at two-loop order in the matter fields. We find that the corrections due to the presence of dynamical gravity are *not* expressible simply in terms of a multiplicative factor as previously obtained at the one-loop level. Our result indicates that the critical points of the theory are nontrivially influenced and modified by the induced gravity.

IFUM-528-FT

May 1996

---

<sup>\*</sup>E-mail address: penati@milano.infn.it

<sup>†</sup>E-mail address: santambrogio@milano.infn.it

<sup>‡</sup>E-mail address: zanon@milano.infn.it

# 1 Introduction

A bosonic string theory can be described by free scalar fields coupled to two-dimensional quantum gravity [1]. If the dimensions of the system are critical ( $d = 26$ ), then the gravitational fields essentially decouple and act as a curved background. If the system is not conformally invariant ( $d \neq 26$ ), gravity becomes dynamical and leads to important modifications of the scaling properties of the matter which it couples to [2], [3].

Recently a number of papers have studied the gravitational dressing of the renormalization group equations for two-dimensional models. In particular it has been shown that the  $\beta$ -function is multiplicatively renormalized at least at one-loop order in the matter fields [4], [5], [6]

$$\beta_G^{(1)} = \frac{\kappa + 2}{\kappa + 1} \beta_0^{(1)} \quad (1.1)$$

where  $\kappa$  is the central charge of the gravitational  $SL(2R)$  Kac-Moody algebra

$$\kappa + 2 = \frac{1}{12} [c - 13 - \sqrt{(1 - c)(25 - c)}] \quad (1.2)$$

and  $\beta_0$  denotes the  $\beta$ -function in the absence of gravity. The above result has been checked in several examples and tested using different quantization methods of gravity [2], [3], [4], [5], [6]. In all cases the multiplicative renormalization factor appeared to be one-loop universal. Beyond lowest order of perturbation theory the one coupling case has been examined [7]: based on considerations in conformal gauge it has been argued that the gravitational dressing of the nextleading order contribution to the  $\beta$ -function is not in the multiplicative form as in eq. (1.1).

The motivation for the present work was to study the problem at the two-loop level in a quantitative manner on a general setting. We have evaluated the gravitational corrections to a bosonic  $\sigma$ -model  $\beta$ -function at two loops in the matter fields. The calculation has been performed following the quantization procedure of refs. [8], [6]. The system is formulated in  $n = 2 - 2\epsilon$  dimensions with the gravitational conformal mode explicitly separated. This provides a natural definition of *conformal* gauge in  $n$  dimensions. The presence of the Liouville field modifies the physical scale with respect to the standard renormalization scale  $\mu$ . Indeed the physical scale is defined through the only dimensionful object in the theory, i.e. the gravitational cosmological term

$$\Lambda_B \int d^n x \sqrt{-g} \quad (1.3)$$

where  $\Lambda_B$  is the bare cosmological constant. The renormalized constant defined by

$$\Lambda_B = \mu^n \Lambda_R Z \quad (1.4)$$

contains in general a divergent renormalization factor  $Z$ . Thus it is clear that, if renormalized by quantum corrections, the gravitational cosmological term acquires an anomalous dimension and it modifies the relevant scale to be used in the calculation of the dressed  $\beta$ -function [4], [6], [9]

$$\beta_G = \frac{\partial \ln \mu}{\partial \ln(\Lambda_R^{-\frac{1}{n}})} \beta \quad (1.5)$$

being  $\beta$  the function which gives the change of the renormalized couplings with respect to the standard mass scale  $\mu$ . In the presence of induced gravity one has  $\beta = \beta_0 + \beta_g$ , having indicated with  $\beta_0$  the contribution to the beta function in the absence of gravity and with  $\beta_g$  the corrections due to the gravity-matter couplings. At one loop in the matter fields and to first order in the semiclassical limit,  $c \rightarrow -\infty$ , it has been shown that  $\beta_g^{(1)} = 0$  so that  $\beta^{(1)} = \beta_0^{(1)}$  [6]. Moreover the prefactor on the r.h.s. of eq. (1.5) has been computed [8] and complete agreement has been obtained at the one-loop order with the expectation in (1.1). We have extended the calculation at the two-loop level in the matter fields: we have found that the multiplicative dressing is not maintained, a rather compelling indication that the gravitational renormalization is not universal and that the fixed points of the theory are nontrivially affected by the surrounding dynamical gravity.

Our paper is organized as follows: in the next section we describe the model and the approach we have followed to perform the calculation. In section three we briefly summarize the results at the one-loop level and illustrate the general procedure for subtraction of infrared divergences. A careful treatment of this problem is crucial for disentangling infrared versus ultraviolet divergences. The gravity dressed two-loop matter contributions are presented in section four. The final section contains some conclusive remarks, while the two appendices give some details of the relevant calculations.

## 2 The model and the general approach

In order to obtain a quantum theory of gravitation in two dimensions, we start using a formulation of the theory in  $n = 2 - 2\epsilon$  dimensions, following closely the work presented in ref. [8]. There it has been shown that within this approach, in the strong coupling regime and in the  $\epsilon \rightarrow 0$  limit, one reproduces the exact results of two-dimensional quantum gravity [2], [3]. We consider in  $n$ -dimension the Hilbert-Einstein action given by

$$S_G = \frac{1}{16\pi G_0} \int d^n x \sqrt{-g} R \quad (2.1)$$

where  $G_0$  denotes the bare gravitational constant. It can be reexpressed in terms of a background metric,  $\hat{g}_{\mu\nu}$ , and quantum fields,  $h_{\mu\nu}$  and  $\Phi$ , defined in such a way that

$$g_{\mu\nu} = \hat{g}_{\mu\rho}(e^h)^\rho_\nu e^{-\frac{\Phi}{\epsilon}} \quad h^\mu_\mu = 0 \quad (2.2)$$

The quantum-gauge invariance under general coordinate transformations is fixed introducing the following gauge-fixing term

$$S_{GF} = -\frac{1}{32\pi G_0} \int d^n x \sqrt{-\hat{g}} \left[ \hat{D}^\nu h_{\mu\nu} - \partial_\mu \Phi \right] \left[ \hat{D}_\rho h^{\mu\rho} - \partial^\mu \Phi \right] \quad (2.3)$$

In (2.3)  $\hat{D}$  is the background covariant derivative and indices are raised and lowered using the background metric. The corresponding ghost action is given by

$$\begin{aligned} S_{ghosts} = & \frac{1}{16\pi G_0} \int d^n x \sqrt{-\hat{g}} \left[ \psi^{*\mu} \hat{D}^\nu \hat{D}_\nu \psi_\mu - \psi^{*\mu} \hat{R}^\nu_\mu \psi_\nu + \right. \\ & \left. + \partial^\nu \Phi \hat{D}_\mu \psi^{*\mu} \psi_\nu - \hat{D}_\sigma h^\nu_\mu \hat{D}_\nu \psi^{*\mu} \psi^\sigma + O(\epsilon^2) \right] \end{aligned} \quad (2.4)$$

Expanding the background around the flat metric, from the quadratic terms in (2.1) and (2.3), one easily obtains the propagators for the quantum fields  $h_{\mu\nu}$  and  $\Phi$

$$\begin{aligned} \langle h_{\mu\nu} h_{\rho\sigma} \rangle &= 16\pi G_0 h_{\mu\nu\rho\sigma} \frac{1}{q^2} \\ \langle \Phi \Phi \rangle &= 16\pi G_0 \frac{2\epsilon}{n} \frac{1}{q^2} \end{aligned} \quad (2.5)$$

where we have defined

$$h_{\mu\nu\rho\sigma} \equiv \delta_{\mu\rho} \delta_{\nu\sigma} + \delta_{\mu\sigma} \delta_{\nu\rho} - \frac{2}{n} \delta_{\mu\nu} \delta_{\rho\sigma} \quad (2.6)$$

Similarly one reads the propagators for the ghosts from the kinetic terms in (2.4).

As mentioned above, adopting this quantization method one can compute the exact scaling exponents of two-dimensional quantum gravity [2], [3], with  $\epsilon \rightarrow 0$  in the strong coupling regime [8]. More precisely, if free matter fields with central charge  $c$  are included, the one-loop counterterm leads to a renormalization of the gravitational coupling constant [8]

$$\frac{1}{G_0} = \mu^{-2\epsilon} \left( \frac{1}{G} - \frac{1}{3} \frac{c-25}{\epsilon} \right) \quad (2.7)$$

where  $\mu$  is the renormalization mass. In the strong coupling limit, i.e.  $|G| \gg |\epsilon|$ , one has

$$\frac{1}{G_0} \sim \mu^{-2\epsilon} \frac{1}{3} \frac{25-c}{\epsilon} \quad (2.8)$$

Now the presence of induced dynamical gravity will counteract matter around. We concentrate on the case of a bosonic  $\sigma$ -model described by the following action

$$S_M = -\frac{1}{4\pi\alpha} \int d^n x \sqrt{-g} g^{\mu\nu} \partial_\mu \phi^i \partial_\nu \phi^j G_{ij}(\phi) \quad (2.9)$$

We want to study the effects of the gravitational interaction on the renormalization group flows of the system and compute the on-shell  $\beta$ -function. To this end it is convenient to use the quantum–background field method and expand the action in normal coordinates [10]

$$\begin{aligned} S_M = & -\frac{1}{4\pi\alpha} \int d^n x \sqrt{-g} g^{\mu\nu} \left[ \partial_\mu \phi^i \partial_\nu \phi^j G_{ij}(\phi) \right. \\ & + 2D_\mu \xi^a \partial_\nu \phi^i E_{ia}(\phi) + D_\mu \xi^a D_\nu \xi^b \delta_{ab} - \partial_\mu \phi^i \partial_\nu \phi^j R_{iab}(\phi) \xi^a \xi^b \\ & - \frac{4}{3} \partial_\mu \phi^i \xi^a \xi^b D_\nu \xi^c R_{caib}(\phi) - \frac{1}{3} \partial_\mu \phi^i \partial_\nu \phi^j \xi^a \xi^b \xi^c D_c R_{iab}(\phi) \\ & - \frac{1}{3} D_\mu \xi^a \xi^b D_\nu \xi^c \xi^d R_{abcd}(\phi) - \frac{1}{2} \xi^a \xi^b \xi^c D_\mu \xi^d \partial_\nu \phi^i D_c R_{daib}(\phi) \\ & \left. - \frac{1}{12} \partial_\mu \phi^i \partial_\nu \phi^j \xi^a \xi^b \xi^c \xi^d (D_a D_b R_{icjd}(\phi) - 4R_{aib}^k(\phi) R_{kcd}(\phi)) + O(\xi^5) \right] \quad (2.10) \end{aligned}$$

where  $\xi^a$  are coordinates in the tangent frame and  $D_\mu \xi^a = \partial_\mu \xi^a + \partial_\mu \phi^i \omega_i{}^{ab}(\phi) \xi_b$ , being  $E_{ia}$  the vielbein and  $\omega_{iab}$  the spin–connection of the target space. The propagator of the quantum fields  $\xi^a$  is

$$\langle \xi^a \xi^b \rangle = 2\pi\alpha \frac{\delta^{ab}}{q^2} \quad (2.11)$$

while the gravity–matter interaction vertices can be obtained from (2.10) using the quantum–background expansion

$$\sqrt{-g} g^{\mu\nu} = \sqrt{-\hat{g}} (e^{-h})_\rho^\mu \hat{g}^{\rho\nu} e^\Phi \quad (2.12)$$

The material we have briefly summarized gives the relevant informations which are needed in order to compute the dressed  $\beta$ -function in the semiclassical limit  $c \rightarrow -\infty$ . In this approximation it suffices to consider contributions with only one quantum gravity line, i.e. only one  $G_0$  factor. More precisely in this limit we have (see eq. (2.8))

$$G_0 \sim -\frac{3}{c} \epsilon \quad (2.13)$$

Therefore in what follows we completely disregard the ghost couplings and the quantum gravity self–interactions. Our general strategy consists in identifying the Feynman diagrams which give rise to divergent integrals, remove infrared divergences, subtract ultraviolet subdivergences and extract the overall divergence. Dimensional regularization is used to evaluate divergent integrals. Infrared infinities are completely removed by an appropriate choice of the subtraction procedure which is rather easily implemented at higher loops [11]. Subtraction of subdivergences corresponding to lower–loop renormalizations insures automatic cancellation of non–local infinite contributions, so that the renormalization counterterms correspond to local corrections of the  $\sigma$ –model metric [12]

$$G_{ij}^B = G_{ij}^R + \sum_{k=1}^{\infty} \frac{1}{\epsilon^k} T_{ij}^{(k)}(G^R) \quad (2.14)$$

The coefficient of the  $1/\epsilon$  pole is the relevant one for the  $\beta$ –function computation

$$\beta_{ij}(G^R) = 2\epsilon G_{ij}^R + 2(1 + \lambda \frac{\partial}{\partial \lambda}) T_{ij}^{(1)}(\lambda^{-1} G^R) \Big|_{\lambda=1} \quad (2.15)$$

In the next section we review the results at the one–loop level with special emphasys on the infrared subtraction procedure.

### 3 One–loop dressing and infrared divergences

The perturbative calculation of the  $\beta$ –function for the  $\sigma$ –model in (2.9), in the absence of dynamical gravity, has been performed up to several loop orders and we refer the reader to the relevant literature for a review of the basic, standard methods and techniques [12], [10], [13].

The one–loop contribution is obtained from the ultraviolet divergence of the diagram in fig. 1. It produces the following structure in the effective action

$$\Gamma_{\infty}^{(1)} = \frac{1}{8\pi\epsilon} \int d^n x \sqrt{-\hat{g}} \hat{g}^{\mu\nu} \partial_{\mu} \phi^i \partial_{\nu} \phi^j R_{ij} \quad (3.1)$$

with the Ricci tensor defined as  $R_{kl} \equiv R^i_{\phantom{i}kil}$ .

Radiative gravitational corrections to leading order in the semiclassical limit [6] are computed from diagrams with one  $h_{\mu\nu}$  or one  $\Phi$  insertion. Both gravity propagators contain a  $G_0$  factor; thus from eqs. (2.5), (2.13) we have that the  $h_{\mu\nu}$  line is  $O(\epsilon)$ , while the  $\Phi$  line is  $O(\epsilon^2)$ . This has to be kept in mind when operating subtractions of subleading divergences and isolating the  $1/\epsilon$  divergences from the relevant integrals.

The gravity dressing of the one–loop  $\sigma$ –model  $\beta$ –function is determined from the Feynman diagrams in fig. 2, where the dashed lines denote either the  $h_{\mu\nu}$  or the  $\Phi$

propagator. Other divergent graphs containing at least one tadpole loop are of no interest here: indeed, after subtraction of subdivergences, they do not produce  $1/\epsilon$  poles and thus do not contribute to the  $\beta$ -function. For this same reason divergent diagrams with at least one tadpole will be discarded also at higher-loop level.

The evaluation of the leading divergence of the various contributions from fig. 2 is rather simple. Even the removal of infrared divergences does not present technical difficulties to this loop order: it can be implemented easily using different but equivalent methods. However, at higher-loop level, we have found advantageous to adopt an infrared regularization [11] which essentially parallels the BPHZ subtraction method for ultraviolet divergences. The idea is to use a procedure which completely removes infrared infinities from any given integral. Consequently we are free to modify the various diagrams (even changing their infrared behaviour), as long as we do not alter their ultraviolet divergent nature. This allows for example to evaluate all the graphs at zero external momenta and/or route an external momentum through the graph in some convenient way [14], [15]. In so doing the infrared divergences will be rearranged, but we need not worry since in the end they will all be removed.

We illustrate this method on a simple example and compute in detail the contribution from the diagram in fig. 2a, with the dashed line denoting the  $h_{\mu\nu}$  propagator. One obtains a contribution proportional to  $h^{\mu\rho\nu\sigma} I_{\mu\nu\rho\sigma}$  with  $I_{\mu\nu\rho\sigma}$  given by the following integral

$$I_{\mu\nu\rho\sigma} = G_0 \int d^n q \, d^n r \, \frac{q_\mu q_\nu (q-r)_\rho (q-r)_\sigma}{(q^2)^2 (q-r)^2 r^2} \quad (3.2)$$

In order to keep the notation manageable in the main text, we use the convention of dropping factors of  $(2\pi)^{-n}$  for each loop integral, with the understanding that at the end we will have to reinsert a factor  $(4\pi)^{-\frac{n}{2}}$  for each loop. The reader can find in the Appendices the relevant formulas with all the factors spelled out. Using the first IR subtraction formula listed in Appendix A, eq. (A.2), one easily performs the  $r$ -integral

$$\begin{aligned} \int d^n r \frac{(q-r)_\rho (q-r)_\sigma}{(q-r)^2 r^2} &\rightarrow \int d^n r \frac{(q-r)_\rho (q-r)_\sigma}{(q-r)^2 r^2} + \frac{1}{\epsilon} \frac{q_\rho q_\sigma}{q^2} = \\ &= (1+2\epsilon) \left\{ \frac{1}{2\epsilon} \frac{\delta_{\rho\sigma}}{(q^2)^\epsilon} - \frac{1-\epsilon}{\epsilon} \frac{q_\rho q_\sigma}{(q^2)^{1+\epsilon}} \right\} + \frac{1}{\epsilon} \frac{q_\rho q_\sigma}{q^2} + O(\epsilon) \end{aligned} \quad (3.3)$$

Then the integration over the  $q$ -variable leads to

$$I_{\mu\nu\rho\sigma} \sim G_0 \left[ \frac{1}{16\epsilon^2} \left( 1 + \frac{\epsilon}{2} \right) 3\delta_{(\mu\nu}\delta_{\rho\sigma)} + \frac{1}{8\epsilon^2} (1+3\epsilon) \delta_{\mu\nu}\delta_{\rho\sigma} \right] \quad (3.4)$$

where, in order to handle infrared subtractions, use of (A.3) and (A.4) has been made. Since  $G_0 = O(\epsilon)$  only the second order poles in eq. (3.4) are relevant. Now we must

subtract subleading ultraviolet divergences. The only divergent sub-diagram is the one which does not contain the gravity propagator (the loop containing the  $h_{\mu\nu}$  line gives  $O(G_0/\epsilon) \sim O(1)$  finite contributions). Therefore we concentrate on the  $q$ -loop. Setting  $r = 0$  we find

$$\left[ \int d^n q \frac{q_\mu q_\nu q_\rho q_\sigma}{(q^2)^3} \right]_{div} = \frac{1}{8\epsilon} 3\delta_{(\mu\nu} \delta_{\rho\sigma)} \quad (3.5)$$

Once again we have used eq. (A.4). Thus to eq. (3.4) one must add the following divergent contribution

$$- \frac{1}{8\epsilon} 3\delta_{(\mu\nu} \delta_{\rho\sigma)} G_0 \int d^n r \frac{1}{r^2} = - \frac{1}{8\epsilon^2} 3\delta_{(\mu\nu} \delta_{\rho\sigma)} G_0 \quad (3.6)$$

Finally, using the identities in Appendix A, namely eqs. (A.11, A.12), one finds

$$h^{\mu\rho\nu\sigma} I_{\mu\nu\rho\sigma} \rightarrow G_0 \left[ -\frac{1}{16\epsilon^2} 8 + \frac{1}{8\epsilon^2} 4 \right] = 0 \quad (3.7)$$

so that the diagram in fig. 2 with an  $h_{\mu\nu}$  line does not contribute to the  $\beta$ -function.

One easily reaches the same conclusion when the gravity insertion corresponds to a  $\Phi$  line. In this case the propagator is  $O(\epsilon^2)$  so that it cancels the  $1/\epsilon^2$  poles from the loop integrations and no divergent contributions survive.

The integrals corresponding to the diagrams in fig. 2b, 2c can be evaluated in similar manner. It is straightforward to show that both contributions separately vanish so that, as anticipated in the introduction, one finds [6]

$$\beta_g^{(1)} = 0 \quad (3.8)$$

At one-loop order in the  $\sigma$ -model fields the gravitational dressing is simply given by the multiplicative factor from the cosmological constant renormalization. Now we turn to the next order in perturbation theory.

## 4 Gravitational corrections to two-loop matter

We consider the gravitational dressing of the two-loop matter  $\beta$ -functions. The standard two-loop  $\beta$ -function without gravity is obtained from the divergences of the diagram in fig. 3. The corresponding contribution to the effective action is given by

$$\Gamma_\infty^{(2)} = \frac{\alpha}{32\pi\epsilon} \int d^n x \sqrt{-\hat{g}} \hat{g}^{\mu\nu} \partial_\mu \phi^i \partial_\nu \phi^j R_{iklm} R_j^{klm} \quad (4.1)$$

In order to evaluate corrections due to the presence of dynamical gravity in the semi-classical limit we need consider all possible two-loop matter graphs with the insertion of

one  $h_{\mu\nu}$  or one  $\Phi$  propagator. The corresponding, various contributions can be grouped on the basis of the background structures they end up being proportional to. In order to write the answer in terms of independent tensors we make use of the following relation

$$D^a D^b R_{iab} = -R_i^a R_{ja} + R_{iab} R^{ab} + D^a D_a R_{ij} - \frac{1}{2} D_i D_j R \quad (4.2)$$

Moreover we drop the term  $D_i D_j R$  since it gives rise to a contribution in the effective action which vanishes on-shell. In so doing we can assemble the total sum of terms relevant for the  $\beta$ -function calculation in the form

$$\frac{\alpha}{12\pi} \frac{G_0}{\epsilon^2} \int d^n x \sqrt{-\hat{g}} \hat{g}^{\mu\nu} \partial_\mu \phi^i \partial_\nu \phi^j (a_1 R_{iklm} R_j^{klm} + a_2 R_{ikjl} R^{kl} + a_3 R_{ik} R_j^k + a_4 D^k D_k R_{ij}) \quad (4.3)$$

with the numerical coefficients  $a_i$  to be determined by the explicit evaluation of the relevant Feynman diagrams. From the action in eq. (2.10) it is easy to see how the structures in eq. (4.3) are produced from graphs which combine in various ways the quantum–background vertices. In figs. 4, 5, 6 we have drawn all the interesting topologies: they give non-vanishing contributions respectively to the  $a_1, a_2, a_3$  coefficients, while the structure proportional to  $a_4$  is produced by a diagram like the one in fig. 6a. As mentioned earlier graphs containing at least one tadpole have not been included since they do not contribute to the  $1/\epsilon$  pole.

As an example of three-loop calculation we give details of the evaluation of the diagram in fig. 4a with a  $h_{\mu\nu}$  gravity correction. To start with there are four different integrals associated with this diagram, according to the four distinct ways to contract the fields. By integration by parts they can be reduced to the two structures schematically shown in fig. 7, where the arrows denote derivatives acting on the corresponding propagators. We concentrate on the calculation of the loop integrals for the diagram in fig. 7a. Inserting the appropriate combinatoric factor, the contribution from this diagram is

$$\frac{9\alpha}{\pi} h^{\rho\sigma\tau\pi} J_{\mu\nu\rho\sigma\tau\pi} \hat{g}^{\mu\gamma} \hat{g}^{\nu\delta} \partial_\gamma \phi^i \partial_\delta \phi^j R_{iklm} R_j^{klm} \quad (4.4)$$

where

$$J_{\mu\nu\rho\sigma\tau\pi} \equiv G_0 \int d^n k \, d^n q \, d^n r \frac{k_\mu (k-q)_\nu q_\rho (q-r)_\sigma q_\tau (q-r)_\pi}{k^2 (k-q)^2 (q^2)^2 (q-r)^2 r^2} \quad (4.5)$$

We can easily perform the  $k$ -integration in eq. (4.5) using the results (B.3, B.4) listed in Appendix B. We obtain

$$\begin{aligned} J_{\mu\nu\rho\sigma\tau\pi} &= G_0 (1 + 2\epsilon) \left\{ \frac{1}{2\epsilon} \delta_{\mu\nu} \int d^n q d^n r \frac{q_\rho (q-r)_\sigma q_\tau (q-r)_\pi}{(q^2)^{2+\epsilon} (q-r)^2 r^2} \right. \\ &\quad \left. - \int d^n q d^n r \frac{q_\mu q_\nu q_\rho (q-r)_\sigma q_\tau (q-r)_\pi}{(q^2)^{3+\epsilon} (q-r)^2 r^2} \right\} \end{aligned} \quad (4.6)$$

As a second step we evaluate the  $r$ –integral. We make use of eqs. (B.2, B.3, B.4) for the momentum integrals and of the relation in (A.2) for the removal of the infrared divergence

$$\begin{aligned}
J_{\mu\nu\rho\sigma\tau\pi} &= G_0(1+4\epsilon) \left\{ \frac{1}{4\epsilon^2} \delta_{\mu\nu} \delta_{\sigma\pi} \int d^n q \frac{q_\rho q_\tau}{(q^2)^{2+2\epsilon}} \right. \\
&\quad - \frac{1-\epsilon}{2\epsilon^2} \delta_{\mu\nu} \int d^n q \frac{q_\rho q_\sigma q_\tau q_\pi}{(q^2)^{3+2\epsilon}} - \frac{1}{2\epsilon} \delta_{\sigma\pi} \int d^n q \frac{q_\mu q_\nu q_\rho q_\tau}{(q^2)^{3+2\epsilon}} \\
&\quad \left. + \frac{1-\epsilon}{\epsilon} \int d^n q \frac{q_\mu q_\nu q_\rho q_\sigma q_\tau q_\pi}{(q^2)^{4+2\epsilon}} \right\} \\
&\quad + (1+2\epsilon) \left\{ \frac{1}{2\epsilon^2} \delta_{\mu\nu} \int d^n q \frac{q_\rho q_\sigma q_\tau q_\pi}{(q^2)^{3+\epsilon}} - \frac{1}{\epsilon} \int d^n q \frac{q_\mu q_\nu q_\rho q_\sigma q_\tau q_\pi}{(q^2)^{4+\epsilon}} \right\} \quad (4.7)
\end{aligned}$$

Finally the  $q$ –integration is readily done with the help of the infrared prescriptions in eqs. (A.3, A.4, A.5). The result is

$$\begin{aligned}
J_{\mu\nu\rho\sigma\tau\pi} &= G_0 \left[ \frac{1}{24\epsilon^3} (1+5\epsilon) \delta_{\mu\nu} \delta_{\sigma\pi} \delta_{\rho\tau} + \frac{1}{96\epsilon^3} (1+\frac{3}{2}\epsilon) \delta_{\mu\nu} 3\delta_{(\rho\sigma} \delta_{\tau\pi)} \right. \\
&\quad \left. - \frac{1}{48\epsilon^2} \delta_{\sigma\pi} 3\delta_{(\mu\nu} \delta_{\rho\tau)} - \frac{1}{288\epsilon^2} 15\delta_{(\mu\nu} \delta_{\rho\sigma} \delta_{\tau\pi)} \right] \quad (4.8)
\end{aligned}$$

Now we consider UV subdivergences that, if present, we need subtract from the expression in (4.8). At one loop the only subdvergence comes from one of the sub–diagrams which do not contain the gravity line, i.e. the one given by the  $k$ –integral. Power counting would single out another potential subdvergence associated to the  $r$ –integral: in fact this loop, containing the  $h_{\mu\nu}$  gravity propagator, is effectively  $O(G_0/\epsilon)$  and thus it gives rise to a finite contribution. The divergence from the  $k$ –integral is  $\delta_{\mu\nu}(2\epsilon)^{-1}$  and the corresponding one–loop subtraction is given by

$$\begin{aligned}
-\frac{\delta_{\mu\nu}}{2\epsilon} G_0 \int d^n q d^n r \frac{q_\rho (q-r)_\sigma q_\tau (q-r)_\pi}{(q^2)^2 (q-r)^2 r^2} &= \\
= -\frac{1}{16\epsilon^3} (1+3\epsilon) \delta_{\mu\nu} \delta_{\sigma\pi} \delta_{\rho\tau} - \frac{1}{32\epsilon^3} (1+\frac{1}{2}\epsilon) \delta_{\mu\nu} 3\delta_{(\rho\sigma} \delta_{\tau\pi)} \quad (4.9)
\end{aligned}$$

At two loops the UV divergence which must be subtracted is the one associated to the  $k$  and  $q$  integrals. Setting  $r = 0$  we write

$$\begin{aligned}
\left[ \int d^n k d^n q \right]_{div} &= \int d^n k d^n q \frac{k_\mu (k-q)_\nu q_\rho q_\sigma q_\tau q_\pi}{k^2 (k-q)^2 (q^2)^3} = \\
&= (1+2\epsilon) \left\{ \frac{1}{2\epsilon} \delta_{\mu\nu} \int d^n q \frac{q_\rho q_\sigma q_\tau q_\pi}{(q^2)^{3+\epsilon}} - \int d^n q \frac{q_\mu q_\nu q_\rho q_\sigma q_\tau q_\pi}{(q^2)^{4+\epsilon}} \right\} \quad (4.10)
\end{aligned}$$

Again the  $q$ –integral is trivially performed using the relations (A.4, A.5) in Appendix A. After subtraction of its own one–loop subdivergence from the  $k$ –loop, it finally gives

$$\left[ \int d^n k d^n q \right]_{sub} = -\frac{1}{32\epsilon^2} (1-\frac{1}{2}\epsilon) \delta_{\mu\nu} 3\delta_{(\rho\sigma} \delta_{\tau\pi)} - \frac{1}{96\epsilon} 15\delta_{(\mu\nu} \delta_{\rho\sigma} \delta_{\tau\pi)} \quad (4.11)$$

In sum, the two-loop subtraction to be performed in eq. (4.8) is given by

$$\begin{aligned} & \left[ \frac{1}{32\epsilon^2} \left( 1 - \frac{1}{2}\epsilon \right) \delta_{\mu\nu} 3\delta_{(\rho\sigma}\delta_{\tau\pi)} + \frac{1}{96\epsilon} 15\delta_{(\mu\nu}\delta_{\rho\sigma}\delta_{\tau\pi)} \right] G_0 \int d^n r \frac{1}{r^2} = \\ &= G_0 \left[ \frac{1}{32\epsilon^3} \left( 1 - \frac{1}{2}\epsilon \right) \delta_{\mu\nu} 3\delta_{(\rho\sigma}\delta_{\tau\pi)} + \frac{1}{96\epsilon^2} 15\delta_{(\mu\nu}\delta_{\rho\sigma}\delta_{\tau\pi)} \right] \end{aligned} \quad (4.12)$$

(We note that the other two-loop integral in the  $k$  and  $r$  variables is finite after subtraction of its one-loop  $k$  subdivergence.)

Adding the results in eqs. (4.8), (4.9), (4.12) and contracting the various structures with  $h^{\rho\sigma\tau\pi}$  as indicated in eq. (4.4), one can check that the contribution from the graph in fig. 7a with a gravity  $h_{\mu\nu}$  correction is zero. The diagram in fig. 7b can be evaluated following the same procedure. Its contribution to the  $a_1$  coefficient in eq. (4.3) is 1/4.

In an analogous way one can compute the  $1/\epsilon$  divergences from the two diagrams in fig. 7 when a  $\Phi$  propagator is inserted. Again the first graph gives a vanishing contribution, while the second one exactly cancels the corresponding  $h_{\mu\nu}$  correction.

We are now ready to list the results for all the diagrams contributing to the expression in eq. (4.3). Each graph receives several contributions stemming from the different ways of arranging derivatives at the vertices. Integration by parts is used repeatedly in order to obtain an independent set of configurations. For each graph we list the total contribution to the coefficients  $a_i$ , keeping distinct the correction from the  $h_{\mu\nu}$  and the  $\Phi$  propagator.

## 4.1 Contributions proportional to the Riemann–Riemann structure

We present here the results for the diagrams in fig. 4 which all end up producing a background dependence of the form Riemann–Riemann, thus contributing to the  $a_1$  coefficient in (4.3). We have obtained

	$h_{\mu\nu}$	$\Phi$
$4a$ :	$\frac{1}{4}$	$-\frac{1}{4}$
$4b$ :	$-\frac{5}{2}$	$\frac{1}{2}$
$4c$ :	$\frac{1}{6}$	$-\frac{1}{6}$
$4d$ :	$-\frac{13}{12}$	$\frac{1}{12}$
$4e$ :	0	0

$$\begin{array}{lll}
4f & : & \frac{13}{6} \quad -\frac{1}{6} \\
4g & : & 1 \quad \frac{1}{2} \\
4h & : & 0 \quad -\frac{1}{2}
\end{array} \tag{4.13}$$

The total sum is identically zero so that the coefficient  $a_1$  in eq. (4.3) vanishes. Notice in particular that a vanishing result is obtained for the  $h_{\mu\nu}$  and the  $\Phi$  contributions separately.

## 4.2 Contributions proportional to the Riemann–Ricci structure

Here we give the results for the diagrams in fig. 5. In this case the graphs  $c$  and  $d$  with a  $h_{\mu\nu}$  insertion do not contribute, since the tensorial structure of the loop–integrals vanishes when contracted with  $h^{\mu\nu\rho\sigma}$  (see Appendix A eqs. (A.9–A.15)). One obtains

$$\begin{array}{lll}
h_{\mu\nu} & & \Phi \\
\hline
5a & : & -\frac{1}{2} \quad \frac{1}{3} \\
5b & : & \frac{1}{2} \quad 1 \\
5c & : & 0 \quad -1 \\
5d & : & 0 \quad \frac{1}{6}
\end{array} \tag{4.14}$$

Again the sum of the contributions for the  $h_{\mu\nu}$  field is zero, but a nonzero  $a_2$  coefficient for the  $R_{ikjl}R^{kl}$  tensor is produced by the  $\Phi$  coupling.

## 4.3 Contributions proportional to the Ricci–Ricci structure

It is easy to verify that the two diagrams in fig. 6 with a  $h_{\mu\nu}$  insertion do not contribute since, as before, the loop–integrals give a zero result when multiplied by  $h^{\mu\nu\rho\sigma}$ . We have

$$\begin{array}{lll}
h_{\mu\nu} & & \Phi \\
\hline
6a & : & 0 \quad -\frac{1}{2} \\
6b & : & 0 \quad \frac{1}{2}
\end{array} \tag{4.15}$$

and the coefficient  $a_3$  in eq. (4.3) vanishes.

## 4.4 Contributions proportional to the $D^k D_k R_{ij}$ structure

At this point it is an easy task to evaluate the contribution to the coefficient  $a_4$  in eq. (4.3). Indeed all the relevant work has already been done and one simply has to reconsider a diagram with the topology shown in fig. 6a. Last but not least, it gives

$$\begin{array}{ccc}
 h_{\mu\nu} & & \Phi \\
 6a : & 0 & \frac{1}{4}
 \end{array} \tag{4.16}$$

Now an important comment is in order: all the contributions produced at intermediate stages by the coupling of matter to the gravity  $h_{\mu\nu}$  field in the end cancel out completely. This result, expected from a formulation of gravity in two-dimensional conformal gauge, provides a nontrivial check of the general approach and of the actual calculation.

In conclusion the coefficients  $a_2$  and  $a_4$  in (4.3) are nonvanishing and a contribution to the  $\beta$ -function is produced from gravity radiative corrections. We discuss the relevance of this result in the last section.

## 5 Discussion and conclusions

The final answer for the  $\beta$ -function up to two loops follows from a straightforward application of the definition in eq. (2.15)

$$\beta_{ij}^{(1)} + \beta_{ij}^{(2)} = R_{ij} + \frac{\alpha}{2} [R_{iklm} R_j^{klm} - \frac{2}{c} (D^k D_k R_{ij} + 2 R_{ikjl} R^{kl})] \tag{5.1}$$

The remaining gravitational dressing is then obtained multiplying the above expression by the prefactor in the r.h.s. of eq. (1.5). As already mentioned this factor tells how the renormalization mass  $\mu$  changes with respect to the physical scale, which is determined in turn by the renormalization of the cosmological term. It is clear that while at one loop all the informations about the influence of the gravitational fields on the  $\sigma$ -model matter system are contained just in this multiplicative factor, this fails to be true at the two-loop level because of the presence of the last contribution in (5.1). Thus we have found for the  $\sigma$ -model the same pattern as the one suggested for a system with just one coupling constant [7]: beyond leading order in perturbation theory the renormalization group trajectories, and consequently the fixed points are modified significantly by the interaction with the dynamical gravity.

We have performed our calculation using a particular regularization procedure and we have to ask ourselves how the scheme dependence might affect the result we have

presented. The idea is to take into account conventional subtraction ambiguities which would arise from finite subtractions proportional to the one-loop counterterms. Since the quantum–background splitting we have used is non–linear, some care is required [16]: one needs compute the complete set of one-loop counterterms with quantum matter and gravity fields. One can check explicitly that all the counterterm insertions containing a gravity field ( both the ones with  $h_{\mu\nu}$  and the ones with  $\Phi$  ) do not contribute to the  $\beta$ –function, so that the net effect at two loops is the addition to (5.1) of a term proportional to the following expression

$$R_{ik}R_j{}^k - R_{ikjl}R^{kl} - \frac{1}{2}D^kD_kR_{ij} \quad (5.2)$$

This is nothing but the usual dependence on the regularization scheme of the flat two-loop  $\beta$ –function, with no extra corrections due to gravity. One might conclude asserting that the modification of the renormalization group flows is not an artifact of the calculation. It reflects instead the new physics induced by the curved quantum two–dimensional spacetime.

In Ref. [9] the exact dressing of one-loop  $\sigma$ –model  $\beta$ –functions has been obtained for both  $N = 1$  and  $N = 2$  supersymmetric theories coupled to induced supergravity. More precisely it has been shown that for the  $N = 1$  case

$$\beta_G^{(1)} = \frac{\kappa + \frac{3}{2}}{\kappa + 1} \beta_0^{(1)} \quad (5.3)$$

with

$$\kappa + \frac{3}{2} = \frac{1}{8} \left[ c - 5 - \sqrt{(1 - c)(9 - c)} \right] \quad (5.4)$$

while for the  $N = 2$  theory no supergravity dressing is produced for the one-loop  $\beta$ –function. The corresponding analysis at the two–loop level in the matter fields is presently under consideration.

**Acknowledgements:** D. Zanon thanks M. Grisaru for useful conversations. This work has been partially supported by grants no. SC1–CT92–0789 and no. CEE–CHRX–CT92–0035.

## A Infrared counterterms and useful formulae

As emphasized earlier, in our work we had to deal with the typical infrared divergences of massless fields in two dimensions. We have used an infrared regularization procedure

which amounts to regulate directly every infrared divergent factor [11]. For example for each  $1/p^2$  term one introduces a counterterm  $a\delta^{(2)}(p)$  in such a fashion that

$$\int \frac{d^n p}{(2\pi)^n} f(p) \left[ \frac{1}{p^2} - a\delta^{(2)}(p) \right] \quad (\text{A.1})$$

is finite for any test function  $f(p)$  which vanishes at infinity. Choosing in particular  $f(p) = 1/(p^2 + m^2)$  one immediately determines  $a = -\pi/\epsilon$ . Similarly one obtains

$$\frac{1}{(p^2)^{1+(\lambda-1)\epsilon}} \rightarrow \frac{1}{(p^2)^{1+(\lambda-1)\epsilon}} + \frac{\pi}{\lambda\epsilon} \delta^{(2)}(p) \quad (\text{A.2})$$

$$\frac{p_\mu p_\nu}{(p^2)^{2+(\lambda-1)\epsilon}} \rightarrow \frac{p_\mu p_\nu}{(p^2)^{2+(\lambda-1)\epsilon}} + \pi \frac{\delta_{\mu\nu}}{2\lambda\epsilon(1-\epsilon)} \delta^{(2)}(p) \quad (\text{A.3})$$

$$\frac{p_\mu p_\nu p_\rho p_\sigma}{(p^2)^{3+(\lambda-1)\epsilon}} \rightarrow \frac{p_\mu p_\nu p_\rho p_\sigma}{(p^2)^{3+(\lambda-1)\epsilon}} + \pi \frac{3\delta_{(\mu\nu}\delta_{\rho\sigma)}}{4\lambda\epsilon(1-\epsilon)(2-\epsilon)} \delta^{(2)}(p) \quad (\text{A.4})$$

$$\frac{p_\mu p_\nu p_\rho p_\sigma p_\tau p_\pi}{(p^2)^{4+(\lambda-1)\epsilon}} \rightarrow \frac{p_\mu p_\nu p_\rho p_\sigma p_\tau p_\pi}{(p^2)^{4+(\lambda-1)\epsilon}} + \pi \frac{15\delta_{(\mu\nu}\delta_{\rho\sigma}\delta_{\tau\pi)}}{8\lambda\epsilon(1-\epsilon)(2-\epsilon)(3-\epsilon)} \delta^{(2)}(p) \quad (\text{A.5})$$

The ones listed above are all the infrared counterterms that we have used in the evaluation of our diagrams.

In the course of the calculation we made repeated use of some identities that we list here for the convenience of the reader

$$\delta^{\rho\sigma} 3\delta_{(\mu\nu}\delta_{\rho\sigma)} = 4(1 - \frac{1}{2}\epsilon)\delta_{\mu\nu} \quad (\text{A.6})$$

$$\delta^{\tau\pi} 15\delta_{(\mu\nu}\delta_{\rho\sigma}\delta_{\tau\pi)} = 6(1 - \frac{1}{3}\epsilon)3\delta_{(\mu\nu}\delta_{\rho\sigma)} \quad (\text{A.7})$$

$$3\delta^{(\mu\nu}\delta^{\rho\sigma)} 3\delta_{(\mu\nu}\delta_{\rho\sigma)} = 24(1 - \frac{3}{2}\epsilon) \quad (\text{A.8})$$

In addition, with the definition in eq. (2.6) one also obtains

$$\delta_{\mu\nu} h^{\mu\nu\rho\sigma} = 0 \quad (\text{A.9})$$

$$\delta_{\mu\rho} h^{\mu\nu\rho\sigma} = 2(1 - \frac{3}{2}\epsilon)\delta^{\nu\sigma} \quad (\text{A.10})$$

$$\delta_{\mu\rho} \delta_{\nu\sigma} h^{\mu\nu\rho\sigma} = 4(1 - \frac{5}{2}\epsilon) \quad (\text{A.11})$$

$$3\delta_{(\mu\nu}\delta_{\rho\sigma)} h^{\mu\nu\rho\sigma} = 8(1 - \frac{5}{2}\epsilon) \quad (\text{A.12})$$

$$3\delta_{(\mu\nu}\delta_{\rho\sigma)} h^{\mu'\mu\rho\sigma} = 4(1 - \frac{3}{2}\epsilon)\delta^{\mu'}_\nu \quad (\text{A.13})$$

$$3\delta_{(\mu'\nu'}\delta_{\mu\rho)} \delta_{\nu\sigma} h^{\mu\nu\rho\sigma} = 8(1 - 2\epsilon)\delta_{\mu'\nu'} \quad (\text{A.14})$$

$$15\delta_{(\mu'\nu'}\delta_{\mu\rho}\delta_{\rho\sigma)} h^{\mu\nu\rho\sigma} = 24(1 - \frac{11}{6}\epsilon)\delta_{\mu'\nu'} \quad (\text{A.15})$$

## B The basic integrals

We collect in this appendix a list of momentum integrals we have encountered in our calculation. We have used dimensional regularization in the so called G-scheme [15] which is a form of modified minimal subtraction. By introducing a factor  $\Gamma(1 - \epsilon)(4\pi)^{-\epsilon}$  for each loop integral, it leads to the automatic cancellation of irrelevant factors of  $\ln 4\pi$ ,  $\gamma_E$  and  $\zeta(2)$ . We have obtained the following results:

$$\begin{aligned} & \Gamma(1 - \epsilon)(4\pi)^{-\epsilon} \int \frac{d^n k}{(2\pi)^n} \frac{1}{(k^2)^{(\lambda-1)\epsilon} (k-r)^2} = \\ &= \frac{1}{4\pi} \frac{\Gamma(1 - \epsilon) \Gamma(\lambda\epsilon) \Gamma(-\epsilon) \Gamma(1 - \lambda\epsilon)}{\Gamma((\lambda - 1)\epsilon) \Gamma(1 - (\lambda + 1)\epsilon)} \frac{1}{(r^2)^{\lambda\epsilon}} \end{aligned} \quad (\text{B.1})$$

$$\begin{aligned} & \Gamma(1 - \epsilon)(4\pi)^{-\epsilon} \int \frac{d^n k}{(2\pi)^n} \frac{1}{(k^2)^{1+(\lambda-1)\epsilon} (k-r)^2} = \\ &= \frac{1}{4\pi} \frac{\Gamma(1 - \epsilon) \Gamma(1 + \lambda\epsilon) \Gamma(-\epsilon) \Gamma(-\lambda\epsilon)}{\Gamma(1 + (\lambda - 1)\epsilon) \Gamma(-(1 + \lambda)\epsilon)} \frac{1}{(r^2)^{1+\lambda\epsilon}} \end{aligned} \quad (\text{B.2})$$

$$\begin{aligned} & \Gamma(1 - \epsilon)(4\pi)^{-\epsilon} \int \frac{d^n k}{(2\pi)^n} \frac{k_\mu}{(k^2)^{1+(\lambda-1)\epsilon} (k-r)^2} = \\ &= \frac{1}{4\pi} \frac{\Gamma(1 - \epsilon) \Gamma(1 + \lambda\epsilon) \Gamma(-\epsilon) \Gamma(1 - \lambda\epsilon)}{\Gamma(1 + (\lambda - 1)\epsilon) \Gamma(1 - (\lambda + 1)\epsilon)} \frac{r_\mu}{(r^2)^{1+\lambda\epsilon}} \end{aligned} \quad (\text{B.3})$$

$$\begin{aligned} & \Gamma(1 - \epsilon)(4\pi)^{-\epsilon} \int \frac{d^n k}{(2\pi)^n} \frac{k_\mu k_\nu}{(k^2)^{1+(\lambda-1)\epsilon} (k-r)^2} = \\ &= \frac{1}{4\pi} \frac{\Gamma(1 - \epsilon)}{\Gamma(1 + (\lambda - 1)\epsilon) \Gamma(2 - (\lambda + 1)\epsilon)} \frac{1}{(r^2)^{\lambda\epsilon}} \left[ \Gamma(1 + \lambda\epsilon) \Gamma(-\epsilon) \Gamma(2 - \lambda\epsilon) \frac{r_\mu r_\nu}{r^2} \right. \\ & \quad \left. + \frac{1}{2} \Gamma(\lambda\epsilon) \Gamma(1 - \epsilon) \Gamma(1 - \lambda\epsilon) \delta_{\mu\nu} \right] \end{aligned} \quad (\text{B.4})$$

$$\begin{aligned} & \Gamma(1 - \epsilon)(4\pi)^{-\epsilon} \int \frac{d^n k}{(2\pi)^n} \frac{k_\mu k_\nu}{(k^2)^{2+(\lambda-1)\epsilon} (k-r)^2} = \\ &= \frac{1}{4\pi} \frac{\Gamma(1 - \epsilon)}{\Gamma(2 + (\lambda - 1)\epsilon) \Gamma(1 - (\lambda + 1)\epsilon)} \frac{1}{(r^2)^{1+\lambda\epsilon}} \left[ \Gamma(2 + \lambda\epsilon) \Gamma(-\epsilon) \Gamma(1 - \lambda\epsilon) \frac{r_\mu r_\nu}{r^2} \right. \\ & \quad \left. + \frac{1}{2} \Gamma(1 + \lambda\epsilon) \Gamma(1 - \epsilon) \Gamma(-\lambda\epsilon) \delta_{\mu\nu} \right] \end{aligned} \quad (\text{B.5})$$

$$\begin{aligned} & \Gamma(1 - \epsilon)(4\pi)^{-\epsilon} \int \frac{d^n k}{(2\pi)^n} \frac{k_\mu k_\nu k_\rho}{(k^2)^{2+(\lambda-1)\epsilon} (k-r)^2} = \\ &= \frac{1}{4\pi} \frac{\Gamma(1 - \epsilon)}{\Gamma(2 + (\lambda - 1)\epsilon) \Gamma(2 - (\lambda + 1)\epsilon)} \frac{1}{(r^2)^{1+\lambda\epsilon}} \left[ \Gamma(2 + \lambda\epsilon) \Gamma(-\epsilon) \Gamma(2 - \lambda\epsilon) \frac{r_\mu r_\nu r_\rho}{r^2} \right. \\ & \quad \left. + \frac{1}{2} \Gamma(1 + \lambda\epsilon) \Gamma(1 - \epsilon) \Gamma(-\lambda\epsilon) \delta_{\mu\nu} \right] \end{aligned}$$

$$+ \frac{1}{2} \Gamma(1 + \lambda\epsilon) \Gamma(1 - \epsilon) \Gamma(1 - \lambda\epsilon) 3\delta_{(\mu\nu} r_{\rho)} \Big] \quad (\text{B.6})$$

$$\begin{aligned} & \Gamma(1 - \epsilon) (4\pi)^{-\epsilon} \int \frac{d^n k}{(2\pi)^n} \frac{k_\mu k_\nu k_\rho k_\sigma}{(k^2)^{2+(\lambda-1)\epsilon} (k-r)^2} = \\ &= \frac{1}{4\pi} \frac{\Gamma(1 - \epsilon)}{\Gamma(2 + (\lambda-1)\epsilon) \Gamma(3 - (\lambda+1)\epsilon)} \frac{1}{(r^2)^{\lambda\epsilon}} \left[ \Gamma(2 + \lambda\epsilon) \Gamma(-\epsilon) \Gamma(3 - \lambda\epsilon) \frac{r_\mu r_\nu r_\rho r_\sigma}{(r^2)^2} \right. \\ & \quad \left. + \frac{1}{2} \Gamma(1 + \lambda\epsilon) \Gamma(1 - \epsilon) \Gamma(2 - \lambda\epsilon) \frac{6\delta_{(\mu\nu} r_\rho r_{\sigma)}}{r^2} + \frac{1}{4} \Gamma(\lambda\epsilon) \Gamma(2 - \epsilon) \Gamma(1 - \lambda\epsilon) 3\delta_{(\mu\nu} \delta_{\rho\sigma)} \right] \quad (\text{B.7}) \end{aligned}$$

$$\begin{aligned} & \Gamma(1 - \epsilon) (4\pi)^{-\epsilon} \int \frac{d^n k}{(2\pi)^n} \frac{k_\mu k_\nu k_\rho k_\sigma}{(k^2)^{3+(\lambda-1)\epsilon} (k-r)^2} = \\ &= \frac{1}{4\pi} \frac{\Gamma(1 - \epsilon)}{\Gamma(3 + (\lambda-1)\epsilon) \Gamma(2 - (\lambda+1)\epsilon)} \frac{1}{(r^2)^{1+\lambda\epsilon}} \left[ \Gamma(3 + \lambda\epsilon) \Gamma(-\epsilon) \Gamma(2 - \lambda\epsilon) \frac{r_\mu r_\nu r_\rho r_\sigma}{(r^2)^2} \right. \\ & \quad \left. + \frac{1}{2} \Gamma(2 + \lambda\epsilon) \Gamma(1 - \epsilon) \Gamma(1 - \lambda\epsilon) \frac{6\delta_{(\mu\nu} r_\rho r_{\sigma)}}{r^2} + \frac{1}{4} \Gamma(1 + \lambda\epsilon) \Gamma(2 - \epsilon) \Gamma(-\lambda\epsilon) 3\delta_{(\mu\nu} \delta_{\rho\sigma)} \right] \quad (\text{B.8}) \end{aligned}$$

$$\begin{aligned} & \Gamma(1 - \epsilon) (4\pi)^{-\epsilon} \int \frac{d^n k}{(2\pi)^n} \frac{k_\mu k_\nu k_\rho k_\sigma k_\tau}{(k^2)^{3+(\lambda-1)\epsilon} (k-r)^2} = \\ &= \frac{1}{4\pi} \frac{\Gamma(1 - \epsilon)}{\Gamma(3 + (\lambda-1)\epsilon) \Gamma(3 - (\lambda+1)\epsilon)} \frac{1}{(r^2)^{1+\lambda\epsilon}} \left[ \Gamma(3 + \lambda\epsilon) \Gamma(-\epsilon) \Gamma(3 - \lambda\epsilon) \frac{r_\mu r_\nu r_\rho r_\sigma r_\tau}{(r^2)^2} \right. \\ & \quad \left. + \frac{1}{2} \Gamma(2 + \lambda\epsilon) \Gamma(1 - \epsilon) \Gamma(2 - \lambda\epsilon) \frac{10\delta_{(\mu\nu} r_\rho r_\sigma r_\tau)}{r^2} \right. \\ & \quad \left. + \frac{1}{4} \Gamma(1 + \lambda\epsilon) \Gamma(2 - \epsilon) \Gamma(1 - \lambda\epsilon) 15\delta_{(\mu\nu} \delta_{\rho\sigma} r_\tau) \right] \quad (\text{B.9}) \end{aligned}$$

$$\begin{aligned} & \Gamma(1 - \epsilon) (4\pi)^{-\epsilon} \int \frac{d^n k}{(2\pi)^n} \frac{k_\mu k_\nu k_\rho k_\sigma k_\tau k_\pi}{(k^2)^{3+(\lambda-1)\epsilon} (k-r)^2} = \\ &= \frac{1}{4\pi} \frac{\Gamma(1 - \epsilon)}{\Gamma(3 + (\lambda-1)\epsilon) \Gamma(4 - (\lambda+1)\epsilon)} \frac{1}{(r^2)^{1+\lambda\epsilon}} \left[ \Gamma(3 + \lambda\epsilon) \Gamma(-\epsilon) \Gamma(4 - \lambda\epsilon) \frac{r_\mu r_\nu r_\rho r_\sigma r_\tau r_\pi}{(r^2)^3} \right. \\ & \quad \left. + \frac{1}{2} \Gamma(2 + \lambda\epsilon) \Gamma(1 - \epsilon) \Gamma(3 - \lambda\epsilon) \frac{15\delta_{(\mu\nu} r_\rho r_\sigma r_\tau r_\pi)}{(r^2)^2} \right. \\ & \quad \left. + \frac{1}{4} \Gamma(1 + \lambda\epsilon) \Gamma(2 - \epsilon) \Gamma(2 - \lambda\epsilon) \frac{45\delta_{(\mu\nu} \delta_{\rho\sigma} r_\tau r_\pi)}{r^2} \right. \\ & \quad \left. + \frac{1}{8} \Gamma(\lambda\epsilon) \Gamma(3 - \epsilon) \Gamma(1 - \lambda\epsilon) 15\delta_{(\mu\nu} \delta_{\rho\sigma} \delta_{\tau\pi)} \right] \quad (\text{B.10}) \end{aligned}$$

The infrared subtractions in (B.1)-(B.10) can then be performed using (A.2)-(A.5).

## References

- [1] A.M. Polyakov, Phys. Lett. **B103** (1981) 207.
- [2] A.M. Polyakov, Mod. Phys. Lett. **A2** (1987) 893;  
V.G. Knizhnik, A.M. Polyakov and A.B. Zamolodchikov, Mod. Phys. Lett. **A3** (1988) 819.
- [3] F. David, Mod. Phys. Lett. **A3** (1988) 1651;  
J. Distler and H. Kawai, Nucl. Phys. **B321** (1989) 509.
- [4] I.R. Klebanov, I.I. Kogan and A.M. Polyakov, Phys. Rev. Lett. **71** (1993) 3243.
- [5] C. Schmidhuber, Nucl. Phys. **B404** (1993) 342;  
J. Ambjorn and K. Ghoroku, Int. J. Mod. Phys. **9** (1994) 5689.
- [6] Y. Tanii, S. Kojima and N. Sakai, Phys. Lett. **B322** (1994) 59.
- [7] H. Dorn, Phys. Lett. **B343** (1995) 81; HU-BERLIN-EP-95-27, Dec. 1995, hep-th/9512023.
- [8] H. Kawai, Y. Kitazawa and M. Ninomiya, Nucl. Phys. **B393** (1993) 280; **B404** (1993) 684.
- [9] M.T. Grisaru and D. Zanon, Phys. Lett. **B353** (1995) 64.
- [10] L. Alvarez-Gaume', D.Z. Freedman and S. Mukhi, Ann. of Phys. **134** (1981) 85.
- [11] K.G. Chetyrkin and F.V. Tkachov, Phys. Lett. **114B** (1982) 340;  
V.A. Smirnov and K.G. Chetyrkin, Theor. Math. Phys. **63** (1985) 462.
- [12] D. Friedan, Phys. Rev. Lett. **45** (1980) 1057; Ann. of Phys. **163** (1985) 318.
- [13] M.T. Grisaru, A.E.M. van de Ven and D. Zanon, Phys. Lett. **173B** (1986) 423; Nucl. Phys. **B277** (1986) 388, 409.
- [14] A.A. Vladimirov, Theor. Math. Phys. **43** (1980) 417.
- [15] K.G. Chetyrkin, A.L. Kataev and F.V. Tkachov, Nucl. Phys. **B174** (1980) 345;  
K.G. Chetyrkin and F.V. Tkachov, Nucl. Phys. **B192** (1981) 159.
- [16] P.S. Howe, G. Papadopoulos and K.S. Stelle, Nucl. Phys. **B296** (1988) 26.

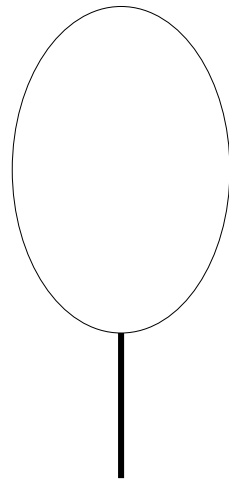


Fig. 1: One loop diagram contributing to the beta function.

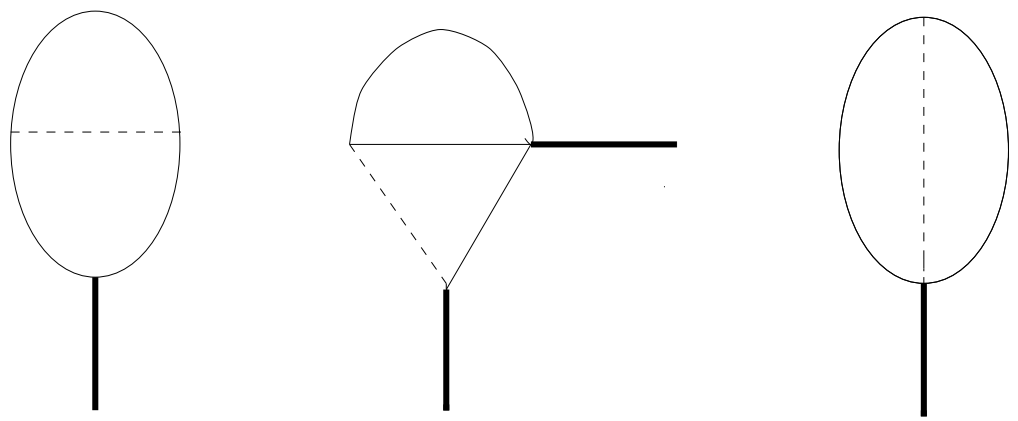


Fig. 2: Divergent diagrams in the presence of gravity. The dashed lines denote gravity propagators.

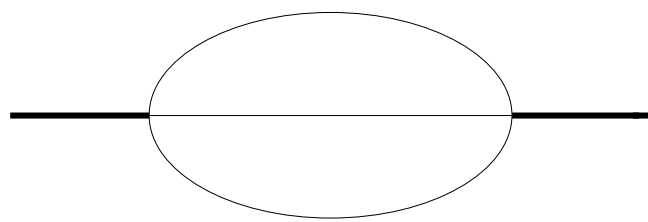
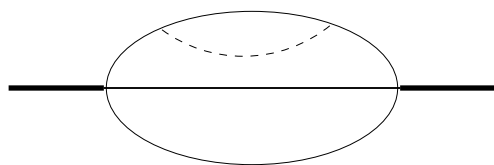
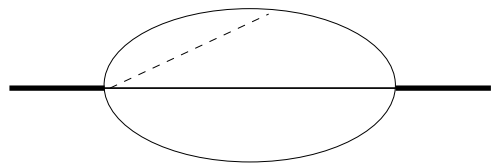


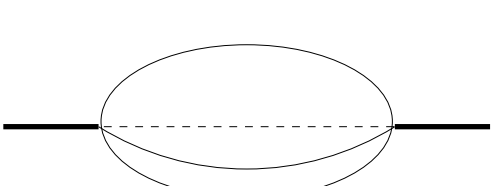
Fig. 3: Two-loop contribution in the absence of gravity.



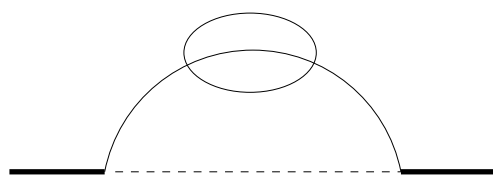
a



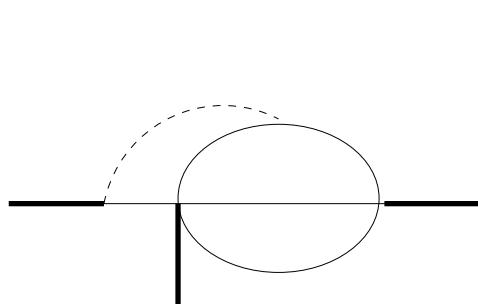
b



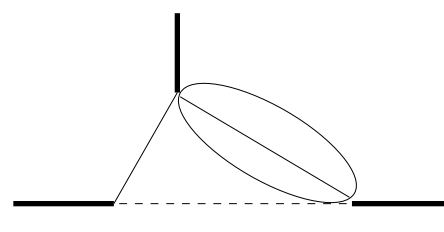
c



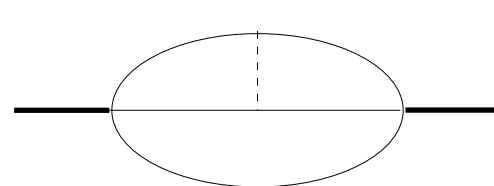
d



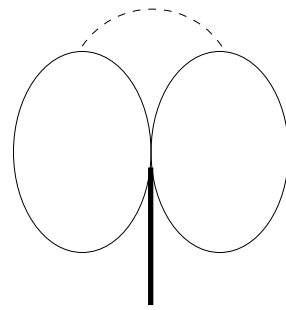
e



f

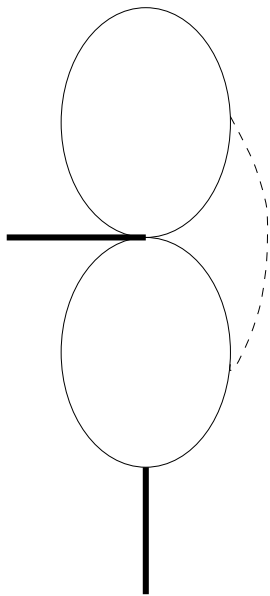


g

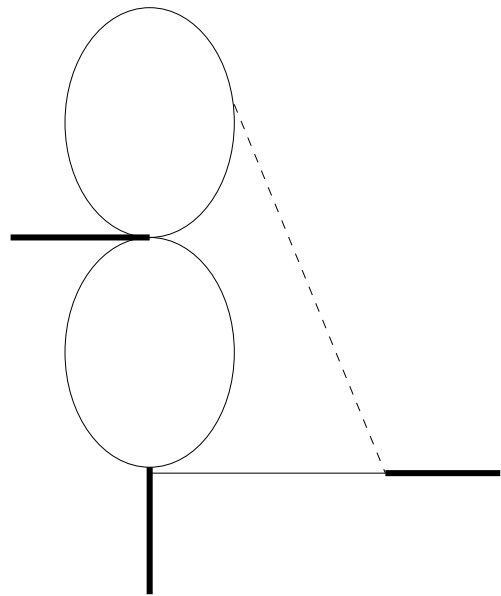


h

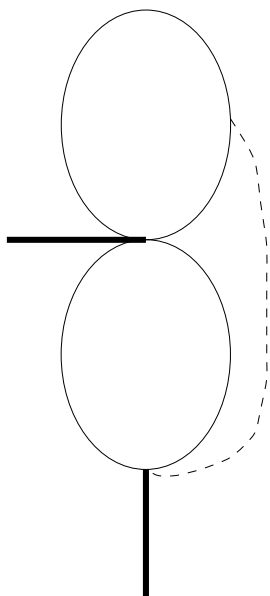
Fig. 4: Diagrams contributing to the Riemann-Riemann structure.



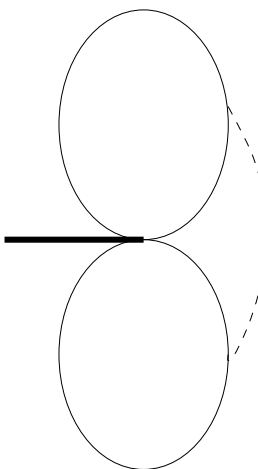
a



b



c



d

Fig. 5: Diagrams contributing to the Riemann-Ricci structure.

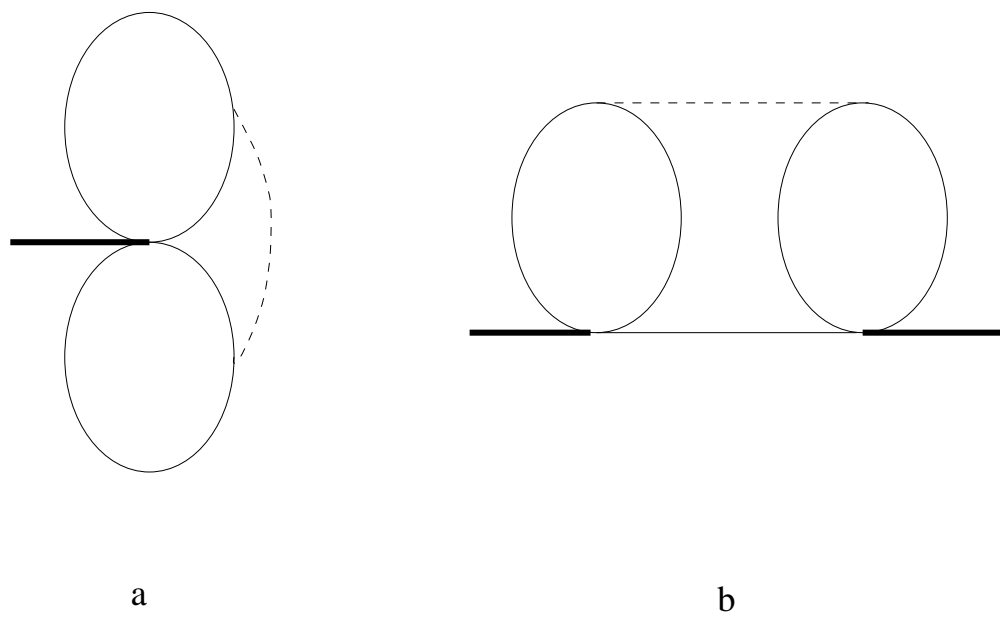
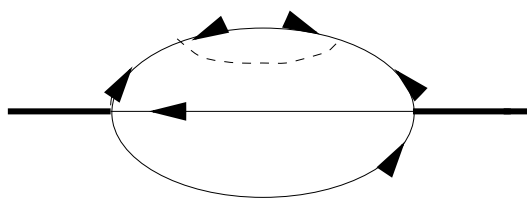
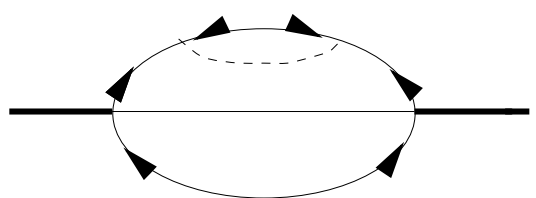


Fig. 6: Diagrams contributing to the Ricci-Ricci structure.



a



b

Fig. 7: An example.